Inlet Diameter and Flow Volume Effects on Separation and Energy Efficiency of Hydrocyclones

Ş Erikli[1, 2], A B Olcay[2]
[1] Dalgakiran Makine A.Ş., Istanbul, Turkey;
[2] Yeditepe University, Mechanical Engineering Department, Atasehir, Istanbul, 34755, Turkey

sukruerikli@dalgakiran.com; bahadir.olcay@yeditepe.edu.tr

Abstract. This study investigates hydrocyclone performance of an oil injected screw compressor. Especially, the oil separation efficiency of a screw compressor plays a significant role for air quality and non-stop working hour of compressors has become an important issue when the efficiency in energy is considered. In this study, two separation efficiency parameters were selected to be hydrocyclone inlet diameter and flow volume height between oil reservoir surface and top of the hydrocyclone. Nine different cases were studied in which cyclone inlet diameter and flow volume height between oil reservoir surface and top were investigated in regards to separation and energy performance aspects and the effect of the parameters on the general performance appears to be causing powerful influence. Flow inside the hydrocyclone geometry was modelled by Reynolds Stress Model (RSM) and hydro particles were tracked by Discrete Phase Model (DPM). Besides, particle break up was modelled by the Taylor Analogy Breakup (TAB) model. The reversed vortex generation was observed at different planes. The upper limit of the inlet diameter of the cyclone yields the centrifugal force on particles to decrease while the flow becomes slower; and the larger diameter implies slower flow. On the contrary, the lower limit is increment in speed causes breakup problems that the particle diameters become smaller; consequently, it is harder to separate them from gas.

1. Introduction

Cyclones known as separators are commonly employed to extract particles or droplets from the system with the help of centrifugal forces. Besides, cyclone structures can be easily manufactured and they have low maintenance and investment costs. While these advantages make the cyclone systems quite popular in the industry, their complex flow characteristics with swirls cannot be solved with mathematical models. Therefore, experimental or numerical approaches have been used to determine the performance of the cyclones. There are many experimental studies regarding to the design of cyclone systems [1] [2] [3]. However, experimental approaches have its own difficulties to identify the flow inside the cyclone since visualization of entire fluid flow inside a closed geometry is very challenging. Hence, observations from inlet and outlet measurements have been typically used to quantify performance parameters of these systems while numerical studies can help to understand the flow characteristics in cyclone systems locally. As a result of improvements in computer processors and solver programs, the time needed to complete a numerical solution has been decreasing; therefore, nowadays many numerical studies [4] [5] [6] related to fluid flow in cyclone systems can be found.

As the fluid flow inside cyclone systems is inherently turbulent, the studies about the turbulence model for swirling flows [6] are investigated. It was realized that the Reynolds Stress Model (RSM) has been widely accepted for swirling flows in these studies while Reynolds Averaged Navier-Stokes (RANS) have been generally employed for fluid flow simulations since this method gives results with reasonable error [7] compared to Large Eddy Simulation (LES) solutions.

In addition to fluid flow simulations in cyclone systems, the particles can be essentially observed with two different methods, namely volume of fluid (VOF) and discrete phase method (DPM). The oil reservoir at the bottom of the oil tank and desired number of particles can be modelled in VOF method with certain restrictions. The limitations in VOF model can be mainly summarized as computational time being longer in VOF than DPM method and VOF method is being unable to model the surface tension or velocity on the droplet surface. On the other hand, DPM is a simulation technique widely used for particle flows and in DPM method particles can be traced and monitored. Furthermore, different particle models such as collision of particles or particle break-ups can be employed. Studies [8] show that the DPM results in cyclone modelling become more accurate with Euler-Lagrangian approach.

When flow characteristics in cyclones and hydrocyclones are considered, gas flow characteristics are observed to be the same for both systems while the particle characteristics show some differences. Particularly, dust cyclones are used for separate solid particles such as dusts while hydrocyclones are utilized for separation of liquids from gas flow. When solid particles flow in the gas phase, there is no change in the shape of solid particles whereas shape of the liquid particle in gas flow can change due to speed, pressure or specification of a gas [9]. However, there is a common challenge for cyclones and hydrocyclones that small particles are typically hard to separate from large particles. There are many studies regarding to dust cyclone geometries and turbulence models used in these studies can be employed for hydrocyclones; however, the studies about particles are not applicable for hydrocyclones. When the fluid flow speed becomes large enough, the liquid droplets break-up and the droplets start to flow as small droplets; as a result, the high speed in hydrocyclones becomes an undesirable situation. On the other hand, collision of solid particles can be interpreted as elastic collisions while the liquid particle collision causes both coalescence and elastic collision. A particle diameter increases after a collision and if the particle diameter passes the already set critical diameter value, the particle may break up to smaller particles. Therefore, the break up and coalescence effects must be considered for hydrocyclones [10]. The breakup effect on separation performance was studied by Gao et al. [11] extensively.

The cyclone geometry was investigated by different researchers. The famous experimental studies based on dust cyclones are examined again with different methods or simulations [5]. Noroozil et al. [12] not only investigated the cyclone inlet diameter effects on cyclone performance, but also the angle of the inlet port of the cyclone. The cyclone main body diameter performance effect on its performance was studied by Yetilmezsoy, 2006 [13].

In this study the inlet diameter and flow volume effects on separation and energy efficiency of hydro cyclones were simulated and investigated. Simulation was based on RANS method. The particles were traced with DPM method and the coalescence and breakup effects were considered. As a result decreasing inlet diameter increases breakup of droplets and the tiny diameters cannot separate from flow and decreasing the diameter of the main [14] body of the cyclone increases the pressure drop. The optimum dimension rate between main body and inlet diameter is tried to be found and discussed.

2. Numerical Model

One of the methods to compress air in industry is to use oil injected screw compressors. In this type of compression, oil is injected into airend to ensure lubrication for rotating screws and provide seal for air leakage (i.e., preventing back flow of air). Once the compression is achieved, oil and air mixture needs to be sent to the hydrocyclones where air is separated from oil. In this study, a simplified numerical model was generated to study performance of separation and energy efficiencies of hydrocyclones. This model was also described and used by Gao et al. (2014) to investigate effects of the central channel on the flow field in an oil-gas hydrocyclones. In this study, three dimensional hydrocyclone with rectangular inlet has been employed and shown in Figure 1. Parameters to describe the hydrocyclone are given in Table 1.

Table 1 Hydrocyclone geometric parameters

Swirl volume height (H)		2D			2.5D			3D		
Hydrocyclone inlet duct	Height (a)	0.3	0.4	0.5	0.3	0.4	0.5	0.3	0.4	0.5
	Width (b)	0.15	0.15	0.15	0.15	0.15	0.15	0.15	0.15	0.15
	Area (a*b)	0.045	0.06	0.075	0.045	0.06	0.075	0.045	0.06	0.075
Hydrocyclone central duct	Diameter (d)	0.5D			0.5D			0.5D		
	Height (h)	D			D			D		
	Inlet length (L)	D			D			D		
Hydrocyclone diameter (D)		D			D			D		

The numerical model illustrated in Figure 1 was generated with SolidWorks based on the parameters provided in Table 1. Three-dimensional hydrocyclone geometry was imported to ICEM-CFD for meshing (Figure 2). Number of elements were different for each simulated case because geometry was changing from one case to another. Table 2 below provides mesh information of the studied nine different cases. In these models, grid independency is ensured by using Gao et al. (2014) [10]. Briefly, three different swirl volume height (H = 2D, 2.5D, and 3D), with three different hydrocyclone inlet duct sizes (0.15 x 0.3, 0.15 x 0.4 and 0.15 x 0.5) were used to study the effect of separation and energy efficiency of hydrocyclones. In order to observe the effects of inlet diameter and swirl volume height on hydrocyclone performance, nine different combinations from diameter and height sets were created and listed in Table 1. Figure 2 shows the computational grid of the numerical model for swirl volume height is being 3D and height of hydrocyclone inlet duct is being 0.5. Total number of elements is 258,064.

Table 2 Studied cases (total of nine different models was generated for the study).

Swirl volume height (H)	2D			2.5D			3D		
Height of hydrocyclone inlet duct (a)	0.3	0.4	0.5	0.3	0.4	0.5	0.3	0.4	0.5
Number of Cells	203269	206473	203353	226227	229088	245907	255255	257837	258064

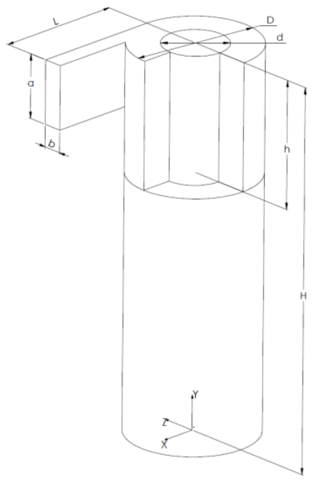

Figure 1. Numerical model with parameters

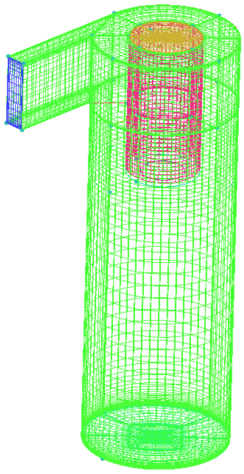

Figure 2. Numerical model with computational grid

Once the meshing was completed, boundary conditions were defined. Pressure and velocity were coupled in equations of motion for incompressible flows. As an outlet boundary condition a static pressure value of pressure outlet was specified while velocity inlet boundary condition was assigned for the inlet. Thus, the velocity at the outlet surface must adjust itself to match the rest of the flow field, similarly at the inlet surface the pressure needs to adjust itself so that the inlet and outlet boundary conditions were not over specified mathematically. DPM particle injection surface was also employed to the inlet surface. In DPM modeling settings, inlet and outlet surfaces were assumed to be an escape boundary condition. All the walls were modeled with no slip boundary wall condition except for the bottom wall. The bottom wall was set to no slip boundary wall condition for turbulence model and trap model for DPM model. Gravity was also defined along -y direction for all simulations. Air and oil material properties were defined for computational grid. Specifically, the air density and viscosity were taken as 3.5 kg/m³ and 2.09×10^{-6} kg/m.s, respectively at 0.2 MPa pressure and the oil density and viscosity were taken as 830 kg/m³ and 5.08 kg/m.s, respectively at 95°C.

There were mainly three assumptions made during this study. First assumption was about the inlet of the cyclone. In this study, a rectangular duct was used instead of a circular pipe. Second assumption was regarding to the oil reservoir. The reservoir oil below the tank was assumed to be a wall with trap condition so that oil surface flow of oil reservoir remained the same. Therefore, the bubble and the returning cached particles would be eliminated. Third assumption was about the shape of the particles. The particles in the study were proposed to be a spherical ball and no change in their shape was allowed during simulations.

In the numerical model the RSM is preferred for the viscous turbulence model. For tracing droplets DPM model was used with sub modules that are Saffman Lift force, Discrete Random Walk (DRW), Breakup, Stochastic Collision and Coalescence. There are a lot of combinations of turbulence solver models for solving different flow problems moderately or decreasing computational time in Fluent. Kaya and Karagöz [6] discusses the best combination for solver models. The most convenient combination was found to be PRESTO for pressure discretization, SIMPLEC for pressure velocity coupling, QUICK for momentum discretization, second-order upwind for turbulent kinetic energy and turbulent dissipation rate and lastly first order upwind for Reynolds stress based on their study. In turbulence modelling, the Reynolds Stress Model (RSM) was utilized to solve Reynolds-averaged Navier-Stokes equations. Although use of RSM increases the computation time of the simulation, this model is typically recommended for cyclone, highly swirling flows in combustors, rotating flow passages, and the stress-induced secondary flow in ducts. Discrete phase model (DPM), utilized in this study, is widely used for the particle flows. In this model particles were added to the flow to track the liquid droplets. The volume fraction of oil particles was generally lower than 10-12% in the flow so that they did not influence the main phase flow of inside the oil tank. The velocity of the particle was dependent on shear force in the particle, main phase velocity and particle. Another additional parameter was about changing velocity of particle is acceleration "a" due to other forces on the particle.

$$\frac{u_p}{dt} = \frac{1}{\tau_p}\left(u - u_p\right) + a \tag{1}$$

After some analytical integration, the particle velocity at new location n+1 was formulated as:

$$u_p^{n+1} = \frac{u_p^n + \Delta t\left(a + \frac{u^n}{\tau_p}\right)}{1 + \frac{\Delta t}{\tau_p}} \tag{2}$$

And the new location was computed with basic location formula of physics.

$$x_p^{n+1} = x_p^n + \frac{1}{2}\Delta t\left(u_p^n + u_p^{n+1}\right) \tag{3}$$

Forces acting on a particle, defines the acceleration of a particle, were formulated with Lagrangian model in Fluent. The acceleration of a particle was basically dependent on a drag force, density difference between main flow and particle, and an additional acceleration force (F_x) where this force played an important role when the density of the main phase was greater than the density of the particle.

$$\frac{u_p}{dt} = F_D\left(u - u_p\right) + \frac{g_x(\rho_p - \rho)}{\rho_p} + F_x \tag{4}$$

$$F_D = \frac{18\mu}{\rho_p \; {}_p^2}\,\frac{C_D Re}{24} \tag{5}$$

$$Re \equiv \frac{\rho d_p |u_p - u|}{\mu} \tag{6}$$

The oil particles have greater density than air; therefore, F_x becomes negligible. The Saffman lift constant is greater than other additional acceleration force terms, so only Saffman lift force was used in the current study.

$$F_x = \vec{F} = \frac{2K v^{1/2} p d_{ij}}{\rho_p \; {}_p\left({}_{lk} d_{kl}\right)^{1/4}}\left(\vec{v} - \vec{v}_p\right) \tag{7}$$

Instantaneous oil droplet velocity to particle observation in turbulent flow was included when DRW model was activated. The DRW model, uses the fluctuating velocity components, is a discrete piecewise constant functions of time:

$$u = \bar{u} + u' \tag{8}$$

As a result of collision of particle, the particle diameter increases. When the particle diameter and its velocity reach to a certain value, the particle may breakup more tiny particles before it is collided again. The collision possibility of a particle with N-1 particles is approximately (1/2) N^2. When two particles collided, they may be coalesced or bounced. The reaction of the collision of two particles can be calculated by a collisional weber number.

$$We_c = \frac{\rho U_{rel}^2 \bar{D}}{\sigma} \tag{9}$$

When two particles collided, the event results in coalescence or elastic collision. There is another type of coalescence that while two particle flows to same direction if they get closer each other below the critical distance they coalescence. The critical offset is dependent to the Weber number and relative radius between particles. The critical offset formulated by O'Rouke [15] on below.

$$b_{crit} = (r_1 + r_2)\sqrt{min(1.0, \frac{2.4f}{We})} \tag{10}$$

The actual collision parameter b equals to$(r_1 + r_2)\sqrt{Y}$. Y is a random number between 0 and 1. If the b_{crit} is greater than the actual b, particules are collided with coalescence. The term f is a related the ratio between particle radius.

$$f\left(\frac{r_1}{r_2}\right) = \left(\frac{r_1}{r_2}\right)^3 - 2.4\left(\frac{r_1}{r_2}\right)^2 + 2.7\left(\frac{r_1}{r_2}\right) \tag{11}$$

O'Rouke [17] claims that the coalescence causes energy loss; therefore, the coalescent particle velocity cannot be calculated because momentum equation but itself would not be enough. The derived expression for the coalescent particle velocity can be computed from:

$$v_1^{'} = \frac{m_1 v_1 + m_2 v_2 + m_2(v_1 + v_2)}{m_1 + m_2}\left(\frac{b - b_{crit}}{r_1 + r_2 - b_{crit}}\right) \tag{12}$$

In oil droplet breakup, Taylor analogy method is used for low-Weber-number injections. As a result weber number less than 100 the TAB model can be applicable. If one of the particle distortion equals the half of the droplet diameter, droplet assumed to be broken up. The break up occurs when y gets higher than 1 and y can be calculated by formula below.

$$y(t) = We_c + e^{-(t/t_d)}\left[(y_0 - We_c)\cos(\omega t) + \frac{1}{\omega}\left(\frac{dy_0}{dt} + \frac{y_0 - We_c}{t_d}\right)\sin(\omega t)\right] \tag{13}$$

3. Results and Discussions

Gao et al. (2014) discusses their simulation and experimental results, so results of the simulation can be compared with the experimental results. The deviation among the current study, experimental and simulation results by Gao's team is in acceptable level. The results provided in Table 3 are also plotted in Figure 2. For the flow with 14.4 m/s velocity the Low-Re Corrections option is enabled.

Table 3 Pressure loss variations with inlet velocity for Gao's experimental and numerical studies and current study

Inlet Velocity (in m/s)	18.10	17.29	16.89	16.30	15.20	14.40
Pressure drop comparison (in Pa)						
Experimental results	4495.3	3711.46	2808.99	2235.87	1861.66	1468.11
Simulation results by Xiang	4299.10	3487.84	2534.73	1913.09	1473.48	1320.43
Simulation results of current study	4239	3382	2645	2144	1529	1510
Deviations in simulation results						

Simulation results by Xiang	4%	6%	10%	14%	21%	10%
Simulation results of current study	6%	9%	6%	4%	18%	-3%

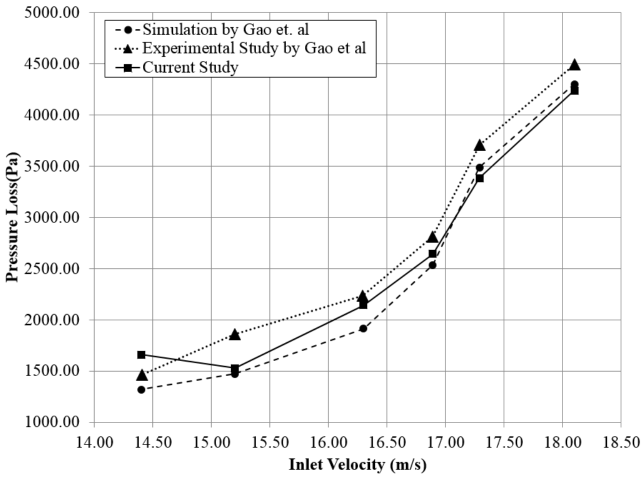

Figure 3. Pressure loss variations with inlet velocity for Gao’s experimental and numerical studies and current study

Tangential velocities on the line parallel to the Z axis at the 75 mm offset from the bottom surface illustrated in Figure 3 show us the central reverse flow swirl channel shape. Besides, it is compared with the simulation results by Gao et al. [10] and they are in acceptable range.

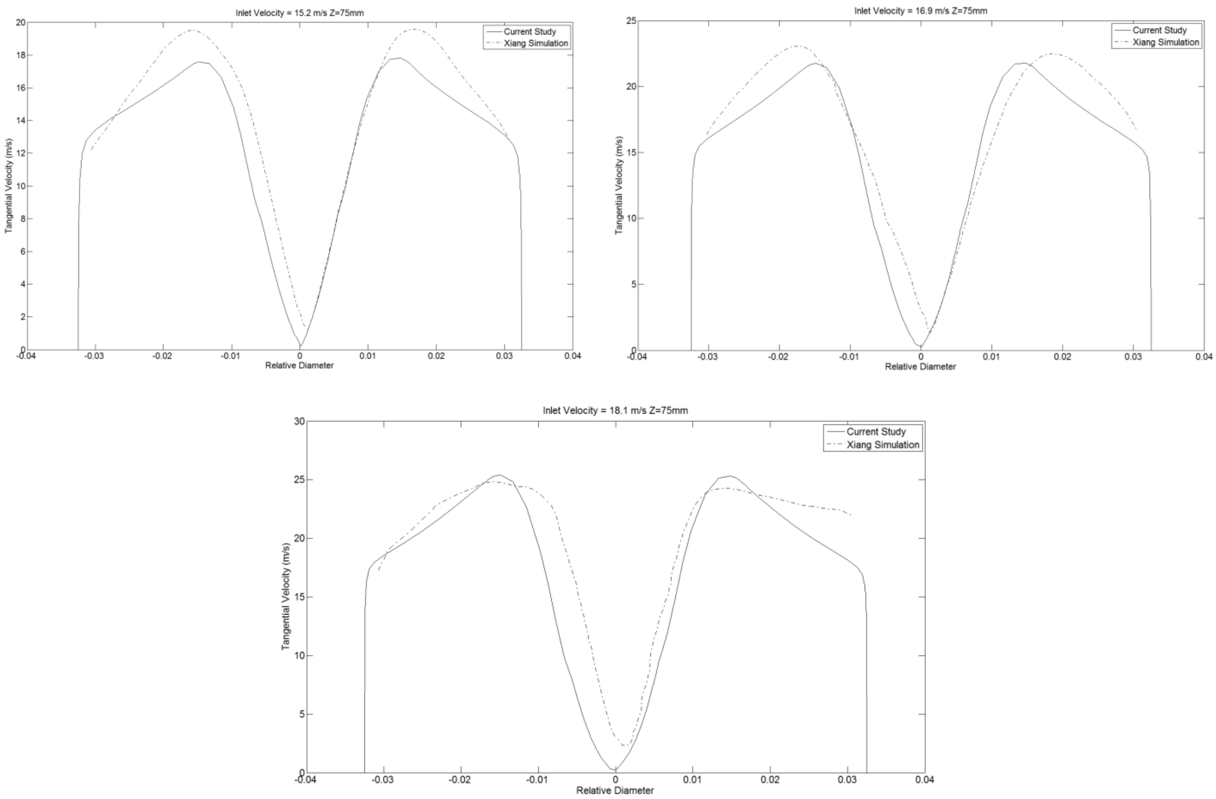

Figure 4. Tangential velocities on the line parallel to the Z axis at the 75 mm offset from y = 0

As a result of high swirl flow velocity the lowest height cyclone has highest pressure lost as shown in Figure 4. Furthermore, for the same volumetric flow rate while inlet diameter is decreasing, flow speed increases therefore it is obvious that the pressure loss increase is inversely proportionally to the inlet diameter.

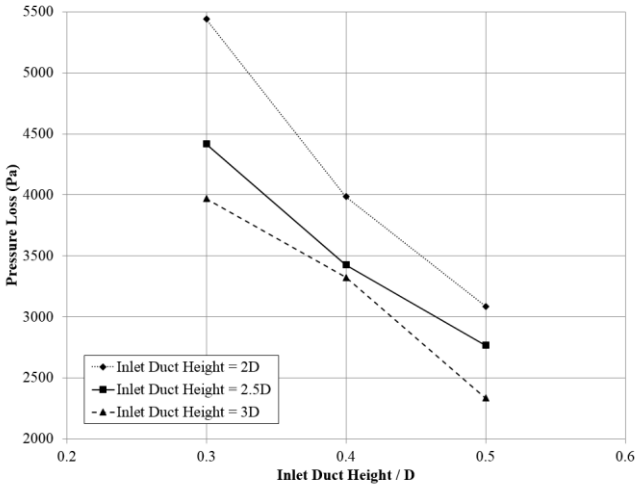

Figure 5. Pressure loss variations with different inlet duct height and swirl volume height

Inlet velocity of the cyclone is known to be effective for the separation performance. The higher inlet velocity causes to increase breakup rate of the particles and the lower inlet velocity slowdowns swirling flow yielding decrease in centrifugal force effect on the particles and decrease in the separation performance. Cyclone height is another effective parameter for the separation; it basically defines the end plane of the swirling flow. The particles flow through the swirling flow and the particles crashes the oil surface at the end of the swirl; therefore, they would be trapped. If the cyclone height is too long, the swirl slows down and more particles would start to discharge from the port. If the cyclone height is too low, there would not be enough time for particles to reach the cyclone surface because particles must flow with swirl. The separation efficiency is calculated from equation 14 below which is a function of total mass of the particles at the inlet and outlet. As a result of breakup and coalescence, the total number of particles may change in flow volume.

$$eff\% = \frac{m_{in} - m_{out}}{m_{in}} \tag{14}$$

Figure 5 shows change of separation efficiency along with inlet duct height. It is noticed that while the cyclone height is increasing from 3D to 2D, separation performance seems to be increasing. On the other hand, for each swirl volume height separation performance shows a decline when inlet duct height is increased. In other words, Figure 5 illustrates that when the inlet diameter decreases, the separation performance shows an increase. Therefore, the separation efficiency increase is inversely proportional with decreasing inlet area.

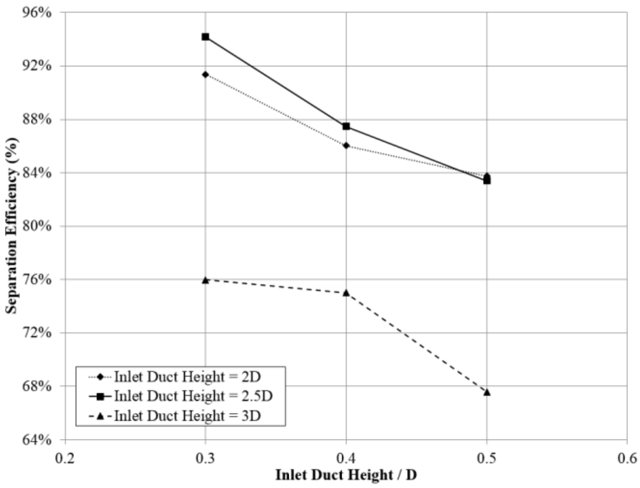

Figure 6. Separation efficiency with different inlet duct height and swirl volume height

4. Conclusions

The optimum point of the separation performance is found to be related with velocities and the flow angles in the cyclone. There are many parameters that can change flow velocity and flow angles. Therefore, prediction of the relation between cyclone geometry and performance is more reliable with performing experiments or simulations.

The height of the cyclone seems to be a significant parameter for separation efficiency and energy consumption. It was noted that while the height is decreasing, the rise of pressure loss is also increased. Another important point is that if the cyclone height is too short, the oil below the tank may be suctioned to the outlet port as a result of low pressure area at the middle of the cyclone. This effect cannot be observed in this study because the oil surface below the tank was assumed to be a surface.

Change in the inlet port diameter seems to be affecting separation efficiency. Specifically, the influence was more for short cyclones than long ones. In short cyclone geometry, the particles are trapped at the bottom surface because swirl changes direction from downward to the upward more sharply in close of bottom trap condition surface. The particles cannot hang on the multiphase flow due to sharp turns and separates. When the bottom surface is closer to the inlet port, the differences of velocities between downward and upward are more from the inlet velocity near the bottom surface, thus increases sharp turn effect.

While the inlet diameter is getting smaller, the separation performance increases the increment rate of the efficiency curve inclination decreasing. Because the high velocity inlet results in more efficient separation, the inlet velocity shows an increase and the breakup possibility of the particles also increases yielding separate particles with 10^{-5} mm diameter.

5. References

[1] J. C. J. F. X. P. Xiang Gao, "Numerical investigation of the effects of the central channel on the flow field in an oil–gas cyclone separator," *Internal Journal of Refrigeration,* no. 36, p. 10, 2013.

[2] Y.-R. C. C.-H. W. R.-M. W. Eldin Wee Chuan Lim, "Experimental and computational studies of multiphase hydrodynamics in a hydrocyclone separator system," *Chemical Engineering Science 65,* 2010.

[3] A.J.Hoekstra, Gas flow field and collection efficiency of cyclone separators, 2000.

[4] J. Gimbun, "Cfd Simulation of Aerocyclone Hydrodynamics and Performance at Extreme Temperature," *Engineering Applications of Computational Fluid Mechanics* , vol. Vol. 2, p. Pp. 22–29, 2008.

[5] D. W. T. N.-M. K. Nageswararao, "Two empirical hydrocyclone models revisited," *Minerals Engineering,* vol. 17, pp. 671-687, 2004.

[6] T. S. Y. C. T. G. C. a. A. F.-R. Jolius Gimbun, "CFD Study on the Prediction of Cyclone Collection Efficiency".

[7] I. K. F.Kaya, "Performance analysis of numerical schemes in highly swirling turbulent flows in cyclones," *Current Science* , vol. 94, no. 10, 2008.

[8] J. D. G. Gronald, "Simulating turbulent swirling flow in a gas cyclone: A comparison of various," *Powder Technology,* vol. 205, pp. 160-171, 2011.

[9] S. R. M. P. B. K. Kozic, "Comparison Of Euler-Euler And Euler-Lagrange Approach In Numerical Simulation Of Multiphase Flow In Ventilation Mill-Air Mixing Duct," *Third Serbian (28th Yu) Congress On Theoretical And Applied Mechanics Vlasina Lake, Serbia, ,* no. B-08, 5-8 July 2011.

[10] R. D. N. T. M. L. Q. E. G. G. M. a. P. V. Utikar, Computational Fluid Dynamics, Hydrodynamic Simulation of Cyclone Separators, H. W. Oh, Ed., InTech, 2010.

[11] "Numerical modelling of droplet break-up for gas atomization," *Computational Materials Science,* vol. 38, p. 282–292, 2006.

[12] Y. Z. X. Y. Y. C. X. P. Xiang Gao, "The Research On The Performance Of Oil-gas Cyclone Separators In Oil Injected Compressor Systems With Considering The Collision And Breakup Of Oil Droplets," *Purdue University Purdue e-Pubs International Compressor Engineering Conference,* no. 2119, p. 10, 2012.

[13] S. H. H. Sooran Noroozi, "CFD Simulation of Inlet Design Effect on Deoiling Hydrocyclone Separation Efficiency," *Chem. Eng. Technol.,* no. No. 12, p. 1885–1893, 2009.

[14] K. Yetilmezsoy, "Determination of Optimum Body Diameter of Air Cyclones Using a New Empirical Model and a Neural Network Approach," *ENVIRONMENTAL ENGINEERING SCIENCE,* vol. 23, no. 4, 2006.

[15] K. N. a. A. L. T.C. RAO, "INFLUENCE OF FEED INLET DIAMETER ON THE HYDROCYCLONE BEHAVIOUR," *International Journal of Mineral Processing,* vol. 3, pp. 357-363, 1976.

[16] J. C. J. F. X. P. Xiang Gao, "umerical and experimental investigations of the effects of the breakup of oil droplets on the performance of oilegas cyclone separators in oil-injected compressor systems," *Computer&Fluids 92,* no. 45-55, p. 10, 2014.

[17] P. B. F. O'Rourke, "Modeling of Drop Interactions in Thick Sprays and a Comparison," *Proceedings of the Institution of Mechanical Engineers,* pp. 101-106, 1980.